Research Paper
Computational Methods for Differential Equations
http://cmde.tabrizu.ac.ir
Vol. *, No. *, *, pp. 1-21
DOI:10.22034/cmde.2024.62630.2773

Investigating soliton solutions and stability analysis in the Riemann wave equation

Hamood Ur Rehman[1,2], **Aamna Amer**[1], **Hameed Ashraf**[1], **Mostafa Eslami**[3,*], **Mohmmad Mirzazadeh**[4,*]

[1]Department of Mathematics, University of Okara, Okara,Pakistan.

[2]Center for Theoretical Physics, Khazar University, 41 Mehseti Street, Baku, AZ1096, Azerbaijan.

[3]Department of Mathematics, Faculty of Mathematical Sciences, University of Mazandaran, Babolsar, Iran.

[4]Department of Engineering Sciences, Faculty of Technology and Engineering, East of Guilan, University of Guilan, Rudsar-Vajargah, P.C. 44891-63157, Iran.

Abstract

The present work aims to investigate solitary wave solutions for the recently developed (2+1)-dimensional Riemann wave equation, which is a significant mathematical model in nonlinear sciences with fascinating applications in fluid dynamics, optics, image processing, plasma physics etc. To analyze this model, we employed four advance techniques- the modified Sardar sub-equation method, new Kudryashov's method, Simplest equation method, and Semi-inverse method to generate several sorts of soliton solutions. A range of categories are encompassed by these solutions, such as periodic, bright solitons, singular solitons, dark solitons, combo bright-singular solitons, exponential, rational, and multi-soliton solutions. The findings reflect the accuracy of the solitary and multi-soliton solutions as well as the effectiveness of the methods. Furthermore, the stability analysis of the solutions is studied for a clearer study of the equations dynamics. To highlight the dynamic behavior and physical importance of the optical soliton solutions of proposed model, several graphical simulations, by three-dimensional (3D) graphs and two-dimensional (2D) plots, are used. This work suggests a major advancement in comprehending the intricate and unpredictable behavior of this model, encouraging readers to explore the world of nonlinear waves and dynamic systems.

Keywords. Riemann wave equation (RWE), Optical Solitons, Modified Sardar sub-equation method (MSSM), New Kudryashov's method (NKM), Hirota solution, Simplest equation method (SEM), Semi-inverse method.

2010 Mathematics Subject Classification. 65L05, 34K06, 34K28.

1. Introduction

Nonlinear evolution equations (NLEEs) are a particular type of partial differential equations (PDEs) that are used in science to describe numerous physical phenomena across diverse disciplines of mathematical and physical sciences, mainely in applied and pure mathematics, physics, chemistry, biology, biochemistry and many other areas [14, 23, 29, 32]. In recent years, researchers have focused on developing more efficient and precise methods for obtaining exact or approximate, analytical or numerical solutions, to nonlinear models [3, 16, 45, 50, 55]. Graphically, these solutions to nonlinear wave equations demonstrate and facilitate the deciphering of the mechanisms behind several complex phenomena. Because NLEEs are high in describing diverse problems across various sectors, researchers are becoming more and more interested in looking for solitary wave solutions [33, 54]. Solitons are particle-like explicit solutions to NPDEs [5, 24, 62]. The most notable technological application of the soliton is the dynamic of pulse propagation for transcontinental trans-oceanic distance through optical fibers. Many scientists have made remarkable efforts to derive traveling wave solutions from such NLPDEs. To carry out exact and explicit stable soliton solutions of nonlinear physical models, several techniques have been devised, such as, extended hyperbolic function method [51], the sub-equation method [6], the tanh-function expansion and its various modifications [15], the Lie

Received: 23 July 2024; Accepted: 08 December 2025.
∗ Corresponding author. Email: mostafa.eslami@umz.ac.ir, mirzazadehs2@guilan.ac.ir.

symmetry analysis [25], the ansatz method [52], the extended rational sine-cosine and rational sinh-cosh method [53], the variational principle [46–48], the complex hyperbolic-function technique [10], the (G'/G^2)-expansion method [34], the variational iteration technique [27], the extended Tanh-Coth method [44], the $(G'/G, 1/G)$-expansion approach [56], the first integral method [4], the modified simple equation method [35], the modified Khater method [36], the sine-Gordon expansion (SGE) method [1, 2, 19, 20, 57], the Sardar sub-equation method [30], the generalized auxiliary equation method [7], the Jacobi elliptic function (JEF) method [9], the homotopy analysis method [26], and much more [13, 31, 60].

This article presents and applies the novel MSSM [8], NKM [37], SEM and SVP to obtain exact solutions to the NLEEs in the form of solitons. To the best of our knowledge, all of these methods have not yet been applied to the Riemann wave equation (RWE). Therefore, by implementing the aforesaid methods, explicit and more general soliton with solitary wave solutions of Riemann wave equation are obtained. Exact solutions enable researchers to plan and conduct experiments by creating an environment that is conductive to determining the parameters or functionalities of the NLEEs. Many researchers have recently discovered exact solutions; lumps solutions; general solutions, and the interaction solutions by transformed rational function method, the modified sardar subequation method is applied on some nonlinear PDEs to find solutions. Eventually, there exist numerous techniques to find solutions to nonlinear differential equations, see [17, 21, 49, 59].

In present study, we deal with the generalized breaking soliton equation and its derivation into the Riemann wave equation and focus on how dimensionless quantities play a role in describing the system's physical behavior. The generalized breaking soliton equation is given by [12]:

$$\mathfrak{V}_t + a\mathfrak{V}_{xx} + b\mathfrak{V}_{xy} + c\mathfrak{V}\mathfrak{V}_x + d\mathfrak{V}\mathfrak{V}_y + e\mathfrak{V}\lambda^{-1}\mathfrak{V}_y = 0. \tag{1.1}$$

Here, the constants a, b, c, d, e are dimensionless coefficients that characterize the interaction between the terms. These constants are typically ratios of physical quantities, such as velocities, lengths, or times, and their dimensionless nature ensures that the equation is applicable across different scales.

The λ^{-1} is also dimensionless constant and represents a spectral parameter that yields the multivalued nature of the solution, which comes from the breaking behavior of the soliton. By adding these dimensionless constants, the equation represents the system's essential physical behavior in a generalized way, independent of specific units. This generalization permits the equation to be applied in different physical application with preserving the key characteristics of soliton behavior. The multi-dimensional breaking soliton equation, given by:

$$\begin{aligned} &\mathfrak{V}_t + a\mathfrak{V}_{xx} + b\mathfrak{V}_{xy} + c\mathfrak{V}\mathfrak{V}_x + d\mathfrak{W}\mathcal{U}_x + e\mathfrak{W}\mathcal{U} = 0, \\ &\mathfrak{V}_y = \mathcal{U}_x, \end{aligned} \tag{1.2}$$

changes the above equation into a multi-dimensional framework. The addition of the variable $\mathcal{U}$ gives another layer of interaction in the wave components. The dimensionless quantities a, b, c, d, e ensures that the models behavior remains scale-independent, making it applicable across different physical systems where wave interactions occur. Consider the Riemann wave equation [18] defined by the following

$$\begin{aligned} &\mathfrak{V}_t + l\mathfrak{V}_{xxy} + m\Psi\mathfrak{V}_y + n\mathcal{U}\mathfrak{V}_x = 0, \\ &\mathfrak{V}_y = \mathcal{U}_x, \\ &\mathfrak{V}_x = \Psi_y. \end{aligned} \tag{1.3}$$

The addition of the variables $\mathfrak{V}_x$ and $\mathcal{U}$, multiplied by these dimensionless constants, enables the model to address overlapping solutions and more complex wave behaviors, while preserving the scale-invariant properties, where n, m, and l are also act as dimensionless quantities that govern the interactions between $\mathfrak{V}_x$ and $\mathcal{U}$.

RWE discussed in this article is an interesting nonlinear equation used to explain the tidal and tsunami waves in ocean, river, electro-magnetic waves in transmission lines, ion and magneto-sound waves in plasmas, homogeneous and stationary media *etc.* The nonlinear terms of first equation in Eq. (1.3) provides the stationary wave propagation properties in the frame of physical sense. Kundu *et al.* [38] examined the parametric analysis using the sine-Gordon expansion method (SGEM), Gurevich *et al.* [22] has applied the slow modulation technique, Barman *et al.* [11]

investigated solitary wave solutions of RWE via the generalized Kudryashov method. Let PDE

$$\mathcal{H} = (\Upsilon, \Upsilon_t, \Upsilon_x, \Upsilon_{xx}, ...) = 0, \tag{1.4}$$

where $\mathcal{H}$ is the function of Υ and its derivatives. We assume the traveling wave transformation as;

$$\Upsilon(x, y, t) = \mathfrak{V}(\zeta), \ \zeta = \vartheta x + \lambda y - \sigma t, \tag{1.5}$$

where ϑ and λ are the wave numbers, and σ is the velocity of the traveling wave which is determined later. By inserting the above transformation into Eq. (1.4), we get the following

$$\overline{\mathcal{H}} = (\mathfrak{V}, \mathfrak{V}', \mathfrak{V}'', ...) = 0. \tag{1.6}$$

This article is assembled as follows: detailed description and solutions of MSSM is provided in section 2. Section 3 discussed the new Kudryashov's method to solve the proposed NLEE. SEM is discussed in section 4. In section 5, stability analysis of solutions is studied. While in section 6, semi-inverse method is studied. In section 7 graphical behavior of solutions are discussed, and finally section 8 is concluded by summarizing our findings.

2. Description of MSSM

The MSSM is an influential technique to determine the exact solutions to the NLEEs. By using this technique, a variety of innovative traveling wave solutions of RWE are generated in this article. The outcomes produced through this method are distinct and unique as compared to previous methods.
The solution of Eq. (1.6) is considered as [40]:

$$\mathfrak{V}(\zeta) = \varpi_0 + \sum_{r=1}^{\epsilon} \varpi_r \phi^r(\zeta), \ \varpi_\epsilon \neq 0, \tag{2.1}$$

where $\varpi_r, \ r = 0, 1, ..., \epsilon$ are constants. The integer ϵ can be determined by balancing the nonlinear terms and the highest derivative in Eq. (1.6). Further, the function $\phi(\zeta)$ in Eq. (2.1) satisfies the following equation:

$$(\phi'(\zeta))^2 = \varrho_2 \phi^4(\zeta) + \varrho_1 \phi^2(\zeta) + \varrho_0, \tag{2.2}$$

where ϱ_0, ϱ_1, and ϱ_2 are constants. Now the general solutions for Eq. (2.2) with parameter ρ are presented as follows:
1. If $\varrho_0 = 0$, $\varrho_1 > 0$, and $\varrho_2 \neq 0$, then

$$\phi_1^{\pm}(\zeta) = \pm\sqrt{-\frac{\varrho_1}{\varrho_2}}\ sech(\sqrt{\varrho_1}(\zeta + \rho)), \tag{2.3}$$

$$\phi_2^{\pm}(\zeta) = \pm\sqrt{\frac{\varrho_1}{\varrho_2}}\ csch(\sqrt{\varrho_1}(\zeta + \rho)). \tag{2.4}$$

2. For two constants β_1 and β_2. Let $\varrho_2 = \pm 4\beta_1\beta_2$, $\varrho_1 > 0$, and $\varrho_0 = 0$, we get

$$\phi_3^{\pm}(\zeta) = \pm\frac{4\beta_1\sqrt{\varrho_1}}{(4\beta_1^2 - \varrho_2)\ cosh(\sqrt{\varrho_1}(\zeta + \rho)) \pm (4\beta_1^2 + \varrho_2)\ sinh(\sqrt{\varrho_1}(\zeta + \rho))}. \tag{2.5}$$

3. If $\varrho_0 = \frac{\varrho_1^2}{4\varrho_2}$, $\varrho_1 < 0$, $\varrho_2 > 0$, with constants A_1 and A_2, then

$$\phi_4^{\pm}(\zeta) = \pm\sqrt{-\frac{\varrho_1}{2\varrho_2}}\ tanh(\sqrt{-\frac{\varrho_1}{2}}(\zeta + \rho)), \tag{2.6}$$

$$\phi_5^{\pm}(\zeta) = \pm\sqrt{-\frac{\varrho_1}{2\varrho_2}}\ coth(\sqrt{-\frac{\varrho_1}{2}}(\zeta + \rho)), \tag{2.7}$$

$$\phi_6^{\pm}(\zeta) = \pm\sqrt{-\frac{\varrho_1}{2\varrho_2}}\ (tanh(\sqrt{-2\varrho_1}(\zeta + \rho)) \pm i\ sech(\sqrt{-2\varrho_1}(\zeta + \rho))), \tag{2.8}$$

$$\phi_7^{\pm}(\zeta) = \pm\sqrt{-\frac{\varrho_1}{8\varrho_2}}\ (tanh(\sqrt{-\frac{\varrho_1}{8}}(\zeta + \rho)) + coth(\sqrt{-\frac{\varrho_1}{8}}(\zeta + \rho))), \tag{2.9}$$

$$\phi_8^{\pm}(\zeta) = \pm\sqrt{-\frac{\varrho_1}{2\varrho_2}}\left(\frac{\pm\sqrt{A_1^2+A_2^2} - A_1\ cosh(\sqrt{-2\varrho_1}(\zeta+\rho))}{A_1\ sinh(\sqrt{-2\varrho_1}(\zeta+\rho)) + A_2}\right), \tag{2.10}$$

$$\phi_9^{\pm}(\zeta) = \pm\sqrt{-\frac{\varrho_1}{2\varrho_2}}\left(\frac{cosh(\sqrt{-2\varrho_1}(\zeta+\rho))}{sinh(\sqrt{-2\varrho_1}(\zeta+\rho)) \pm i}\right). \tag{2.11}$$

4. If $\varrho_0 = 0$, $\varrho_1 < 0$, and $\varrho_2 \neq 0$, then

$$\phi_{10}^{\pm}(\zeta) = \pm\sqrt{-\frac{\varrho_1}{\varrho_2}}\ sec(\sqrt{-\varrho_1}(\zeta+\rho)), \tag{2.12}$$

$$\phi_{11}^{\pm}(\zeta) = \pm\sqrt{-\frac{\varrho_1}{\varrho_2}}\ csc(\sqrt{-\varrho_1}(\zeta+\rho)). \tag{2.13}$$

5. If $\varrho_0 = \frac{\varrho_1^2}{4\varrho_2}$, $\varrho_1 > 0$, $\varrho_2 > 0$, and $A_1^2 - A_2^2 > 0$, then

$$\phi_{12}^{\pm}(\zeta) = \pm\sqrt{\frac{\varrho_1}{2\varrho_2}}\ tan(\sqrt{\frac{\varrho_1}{2}}(\zeta+\rho)), \tag{2.14}$$

$$\phi_{13}^{\pm}(\zeta) = \pm\sqrt{\frac{\varrho_1}{2\varrho_2}}\ cot(\sqrt{\frac{\varrho_1}{2}}(\zeta+\rho)), \tag{2.15}$$

$$\phi_{14}^{\pm}(\zeta) = \pm\sqrt{\frac{\varrho_1}{2\varrho_2}}\ (tan(\sqrt{2\varrho_1}(\zeta+\rho)) \pm sec(\sqrt{2\varrho_1}(\zeta+\rho))), \tag{2.16}$$

$$\phi_{15}^{\pm}(\zeta) = \pm\sqrt{\frac{\varrho_1}{8\varrho_2}}\ (tan(\sqrt{\frac{\varrho_1}{8}}(\zeta+\rho)) - cot(\sqrt{\frac{\varrho_1}{8}}(\zeta+\rho))), \tag{2.17}$$

$$\phi_{16}^{\pm}(\zeta) = \pm\sqrt{\frac{\varrho_1}{2\varrho_2}}\left(\frac{\pm\sqrt{A_1^2-A_2^2} - A_1\ cos(\sqrt{2\varrho_1}(\zeta+\rho))}{A_1\ sin(\sqrt{2\varrho_1}(\zeta+\rho)) + A_2}\right), \tag{2.18}$$

$$\phi_{17}^{\pm}(\zeta) = \pm\sqrt{\frac{\varrho_1}{2\varrho_2}}\left(\frac{cos(\sqrt{2\varrho_1}(\zeta+\rho))}{sin(\sqrt{2\varrho_1}(\zeta+\rho)) \pm 1}\right). \tag{2.19}$$

6. If $\varrho_0 = 0$, $\varrho_1 > 0$, then

$$\phi_{18}^{\pm}(\zeta) = \frac{4\varrho_1 e^{\pm\sqrt{\varrho_1}(\zeta+\rho)}}{e^{\pm 2\sqrt{\varrho_1}(\zeta+\rho)} - 4\varrho_1\varrho_2}, \tag{2.20}$$

$$\phi_{19}^{\pm}(\zeta) = \frac{\pm 4\varrho_1 e^{\pm\sqrt{\varrho_1}(\zeta+\rho)}}{1 - 4\varrho_1\varrho_2 e^{\pm 2\sqrt{\varrho_1}(\zeta+\rho)}}. \tag{2.21}$$

7. If $\varrho_0 = \varrho_1 = 0$, and $\varrho_2 > 0$ then

$$\phi_{20}^{\pm}(\zeta) = \pm\frac{1}{\sqrt{\varrho_2}(\zeta+\rho)}. \tag{2.22}$$

8. If $\varrho_0 = \varrho_1 = 0$, and $\varrho_2 < 0$ then

$$\phi_{21}^{\pm}(\zeta) = \pm\frac{i}{\sqrt{-\varrho_2}(\zeta+\rho)}. \tag{2.23}$$

Substituting Eqs. (2.1) and (2.2) into (1.6), afterwards, an algebraic system of equations with unknown variables ϖ_r, ϑ, λ and σ is produced by collecting and setting all of the coefficients of $\phi^r(\zeta)$ to zero. In the end, we solve the relevant set of equations, insert these variables into Eq. (2.1), and use Eqs. (2.3)-(2.23) to get the precise solutions of Eq. (1.4).

2.1. **Determination of solutions.** Here, we implemented the modified Sardar sub-equation method to analyze the stationary soliton solutions to the Riemann wave equation.

Firstly, applying the traveling wave transformation defined by

$$\begin{aligned}\mathfrak{V}(x,y,t) &= \mathfrak{V}(\zeta),\ \zeta = \vartheta x + \lambda y - \sigma t,\\ \mathcal{U}(x,y,t) &= \mathcal{U}(\zeta),\\ \Psi(x,y,t) &= \Psi(\zeta),\end{aligned} \tag{2.24}$$

into the Riemann wave equation (1.3) results into the following ODE;

$$2\lambda l\vartheta^2\mathfrak{V}'' - 2\sigma\mathfrak{V} + (m\vartheta + n\lambda)\mathfrak{V}^2 = 0, \tag{2.25}$$

where

$$\begin{aligned}\mathcal{U}(\zeta) &= \frac{\lambda}{\vartheta}\mathfrak{V},\\ \Psi(\zeta) &= \frac{\vartheta}{\lambda}\mathfrak{V}.\end{aligned} \tag{2.26}$$

Balancing the highest order linear term $\mathfrak{V}''$ and nonlinear term $\mathfrak{V}^2$ in Eq. (2.25) gives $\epsilon = 2$. Then the solution structure (2.1) takes the form

$$\mathfrak{V}(\zeta) = \varpi_0 + \varpi_1\phi(\zeta) + \varpi_2\phi^2(\zeta),\ \varpi_2 \neq 0, \tag{2.27}$$

Inserting the Eq. (2.2) and Eq. (2.27) into Eq. (2.25). The substitution yields a polynomial as $\phi^r(\zeta)$. By collection of terms with similar powers and setting the resulting expression equal to zero, an over-determined system of algebraic equations is obtained as

$$\begin{aligned}&4\lambda\varrho_0 l\vartheta^2\varpi_2 + \lambda n\varpi_0^2 - 2\sigma\varpi_0 + \vartheta m\varpi_0^2 = 0,\\ &2\lambda\varrho_1 l\vartheta^2\varpi_1 + 2\lambda n\varpi_0\varpi_1 - 2\sigma\varpi_1 + 2\vartheta m\varpi_0\varpi_1 = 0,\\ &8\lambda\varrho_1 l\vartheta^2\varpi_2 + \lambda n\varpi_1^2 + 2\lambda n\varpi_0\varpi_2 - 2\sigma\varpi_2 + \vartheta m\varpi_1^2 + 2\vartheta m\varpi_0\varpi_2 = 0,\\ &4\lambda\varrho_2 l\vartheta^2\varpi_1 + 2\lambda n\varpi_1\varpi_2 + 2\vartheta m\varpi_1\varpi_2 = 0,\\ &12\lambda\varrho_2 l\vartheta^2\varpi_2 + \lambda n\varpi_2^2 + \vartheta m\varpi_2^2 = 0.\end{aligned} \tag{2.28}$$

We get the subsequent values of the unknown parameters with the help of Mathematica by solving the above algebraic system.

$$\begin{aligned}&\varpi_0 = \frac{\varrho_1\varpi_2 - \sqrt{\varrho_1^2\varpi_2^2 - 3\varrho_0\varrho_2\varpi_2^2}}{3\varrho_2},\ \varpi_1 = 0,\ m = \frac{-12\lambda\varrho_2 l\vartheta^2 - \lambda n\varpi_2}{\vartheta\varpi_2},\\ &\sigma = \frac{4\lambda l\vartheta^2\sqrt{(\varrho_1^2 - 3\varrho_0\varrho_2)\,\varpi_2^2}}{\varpi_2},\ \varpi_2 = \varpi_2.\end{aligned} \tag{2.29}$$

From the solutions in Eq. (2.29) along with Eqs. (2.3)-(2.23) and (2.27), we determine the novel soliton solutions of Eq. (1.3) in following manner:

1. For $\varrho_0 = 0,\ \varrho_1 > 0$, and $\varrho_2 \neq 0$.

The bright and singular solitons are as follows, respectively:

$$\mathfrak{V}_1^{\pm}(\zeta) = \frac{\varrho_1\varpi_2 - 3\varrho_1\varpi_2\left(\operatorname{sech}\left(\sqrt{\varrho_1}(\rho+\zeta)\right)\right)^2 - \sqrt{(\varrho_1^2 - 3\varrho_0\varrho_2)\,\varpi_2^2}}{3\varrho_2}, \tag{2.30}$$

$$\mathcal{U}_1^{\pm}(\zeta) = \frac{\lambda}{\vartheta}\mathfrak{V}_1^{\pm}(\zeta), \tag{2.31}$$

$$\Psi_1^{\pm}(\zeta) = \frac{\vartheta}{\lambda}\mathfrak{V}_1^{\pm}(\zeta). \tag{2.32}$$

$$\mathfrak{V}_2^{\pm}(\zeta) = \frac{\varrho_1\varpi_2 + 3\varrho_1\varpi_2\left(\operatorname{csch}\left(\sqrt{\varrho_1}(\rho+\zeta)\right)\right)^2 - \sqrt{(\varrho_1^2 - 3\varrho_0\varrho_2)\,\varpi_2^2}}{3\varrho_2}, \tag{2.33}$$

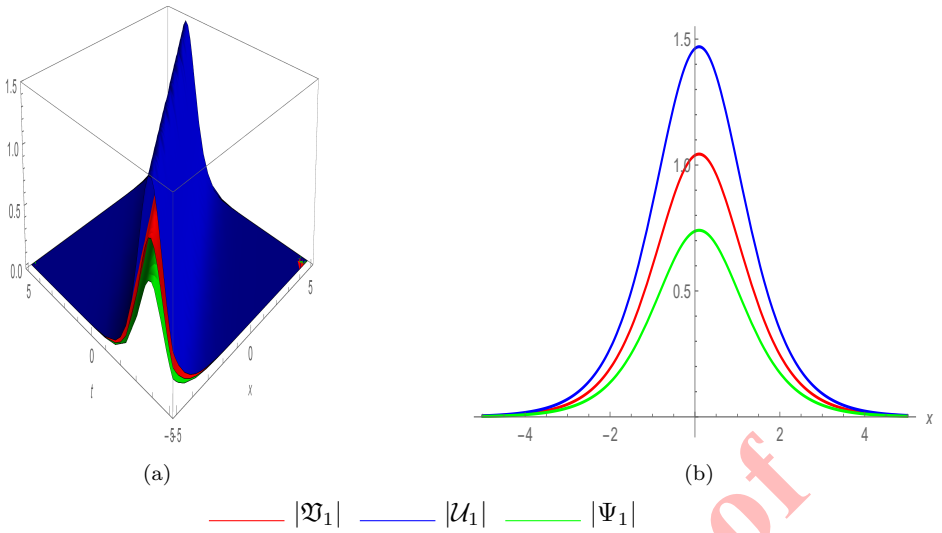

FIGURE 1. Plots of $|\mathfrak{V}_1|$, $|\mathcal{U}_1|$ and $|\Psi_1|$, with $\lambda = -1,\ \varrho_0 = 0,\ \varrho_1 = 1,\ \varrho_2 = 0.92,\ \sigma = 0.98,\ \vartheta = 0.71,\ \rho = 0.84,\ \varpi_2 = 0.96$, and $y = 0.91$. (a) Three-dimensional plot, (b) Two-dimensional plot.

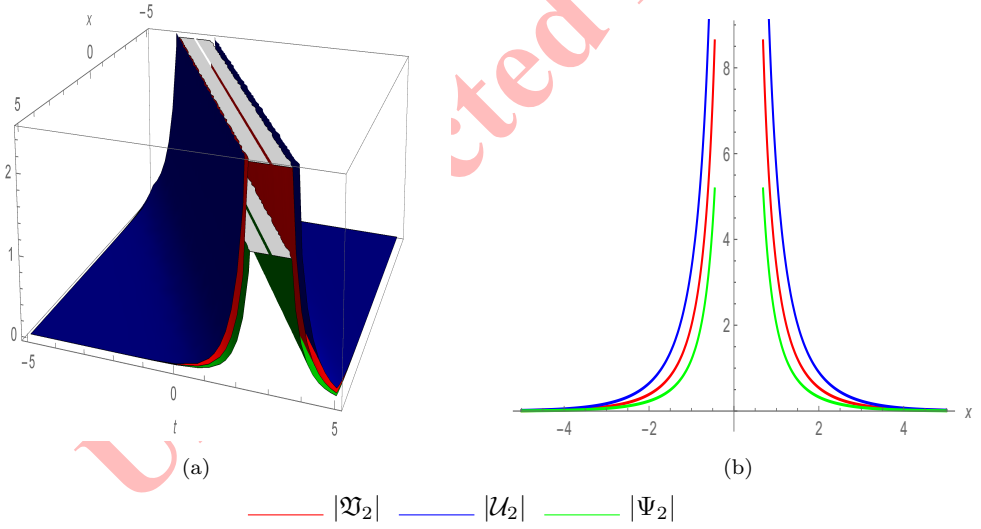

FIGURE 2. Plots of $|\mathfrak{V}_2|$, $|\mathcal{U}_2|$ and $|\Psi_2|$, with $\lambda = -1,\ \varrho_0 = 0, \varrho_1 = 1,\ \varrho_2 = 0.92,\ \sigma = 0.98,\ \vartheta = 0.6,\ \rho = 0.84,\ \varpi_2 = 0.96$ and $y = 0.91$. (a) Three-dimensional plot, (b) Two-dimensional plot.

$$\mathcal{U}_2^{\pm}(\zeta) = \frac{\lambda}{\vartheta}\mathfrak{V}_2^{\pm}(\zeta), \tag{2.34}$$

$$\Psi_2^{\pm}(\zeta) = \frac{\vartheta}{\lambda}\mathfrak{V}_2^{\pm}(\zeta). \tag{2.35}$$

2. For $\varrho_0 = 0,\ \varrho_1 > 0,\ \varrho_2 = \pm 4\beta_1\beta_2$, where $\beta_1,\ \beta_2$ are constants.

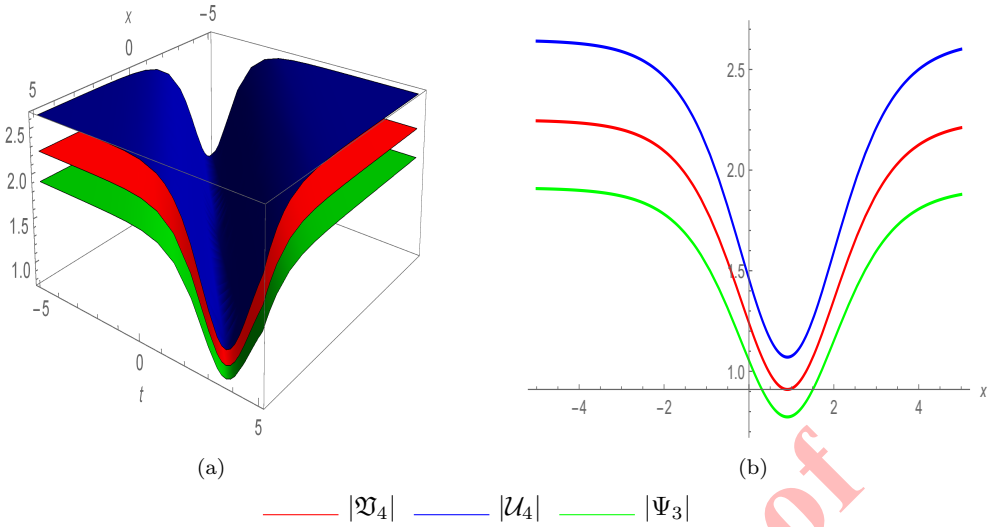

FIGURE 3. Plots of $|\mathfrak{V}_4|$, $|\mathcal{U}_4|$ and $|\Psi_4|$, with $\lambda = -1$, $\varrho_0 = 0.44$, $\varrho_1 = -1$, $\varrho_2 = 0.56$, $\sigma = -0.98$, $\vartheta = -0.85$, $\rho = -0.93$, $\varpi_2 = -1.5$, $\varpi_0 = 0.91$ and $y = -1.7$. (a) Three-dimensional plot, (b) Two-dimensional plot.

The combo of bright-singular solitons is provided as:

$$\mathfrak{V}_3^{\pm}(\zeta) = \frac{1}{3}\left(\frac{48\beta_1^2\varrho_1\varpi_2}{\left((4\beta_1^2-\varrho_2)\cosh\left(\sqrt{\varrho_1}(\rho+\zeta)\right)\pm(4\beta_1^2+\varrho_2)\sinh\left(\sqrt{\varrho_1}(\rho+\zeta)\right)\right)^2} + \frac{\varrho_1\varpi_2-\sqrt{(\varrho_1^2-3\varrho_0\varrho_2)\,\varpi_2^2}}{\varrho_2}\right), \tag{2.36}$$

$$\mathcal{U}_3^{\pm}(\zeta) = \frac{\lambda}{\vartheta}\mathfrak{V}_3^{\pm}(\zeta), \tag{2.37}$$

$$\Psi_3^{\pm}(\zeta) = \frac{\vartheta}{\lambda}\mathfrak{V}_3^{\pm}(\zeta). \tag{2.38}$$

3. For $\varrho_0 = \frac{\varrho_1^2}{4\varrho_2}$, $\varrho_1 < 0$, and $\varrho_2 > 0$.
The dark and other singular solitons are given as:

$$\mathfrak{V}_4^{\pm}(\zeta) = \frac{\varrho_1\varpi_2 - \frac{3}{2}\varrho_1\varpi_2\left(\tanh\left(\frac{\sqrt{-\varrho_1}}{\sqrt{2}}(\rho+\zeta)\right)\right)^2 - \sqrt{(\varrho_1^2-3\varrho_0\varrho_2)\,\varpi_2^2}}{3\varrho_2}, \tag{2.39}$$

$$\mathcal{U}_4^{\pm}(\zeta) = \frac{\lambda}{\vartheta}\mathfrak{V}_4^{\pm}(\zeta), \tag{2.40}$$

$$\Psi_4^{\pm}(\zeta) = \frac{\vartheta}{\lambda}\mathfrak{V}_4^{\pm}(\zeta). \tag{2.41}$$

$$\mathfrak{V}_5^{\pm}(\zeta) = \frac{\varrho_1\varpi_2 - \frac{3}{2}\varrho_1\varpi_2\left(\coth\left(\frac{\sqrt{-\varrho_1}}{\sqrt{2}}(\rho+\zeta)\right)\right)^2 - \sqrt{(\varrho_1^2-3\varrho_0\varrho_2)\,\varpi_2^2}}{3\varrho_2}, \tag{2.42}$$

$$\mathcal{U}_5^{\pm}(\zeta) = \frac{\lambda}{\vartheta}\mathfrak{V}_5^{\pm}(\zeta), \tag{2.43}$$

$$\Psi_5^{\pm}(\zeta) = \frac{\vartheta}{\lambda}\mathfrak{V}_5^{\pm}(\zeta). \tag{2.44}$$

The combo solitons are as follows:

$$\mathfrak{V}_6^{\pm}(\zeta)=\frac{\varrho_1\varpi_2+3\varrho_2\varpi_2\left(\frac{\sqrt{-\frac{\varrho_1}{\varrho_2}}\tanh\left(\left(\sqrt{2}\sqrt{-\varrho_1}\right)(\rho+\zeta)\right)}{\sqrt{2}}\pm i\,\mathrm{sech}\left(\left(\sqrt{2}\sqrt{-\varrho_1}\right)(\rho+\zeta)\right)\right)^2-\sqrt{\left(\varrho_1^2-3\varrho_0\varrho_2\right)\varpi_2^2}}{3\varrho_2}, \tag{2.45}$$

$$\mathcal{U}_6^{\pm}(\zeta)=\frac{\lambda}{\vartheta}\mathfrak{V}_6^{\pm}(\zeta), \tag{2.46}$$

$$\Psi_6^{\pm}(\zeta)=\frac{\vartheta}{\lambda}\mathfrak{V}_6^{\pm}(\zeta). \tag{2.47}$$

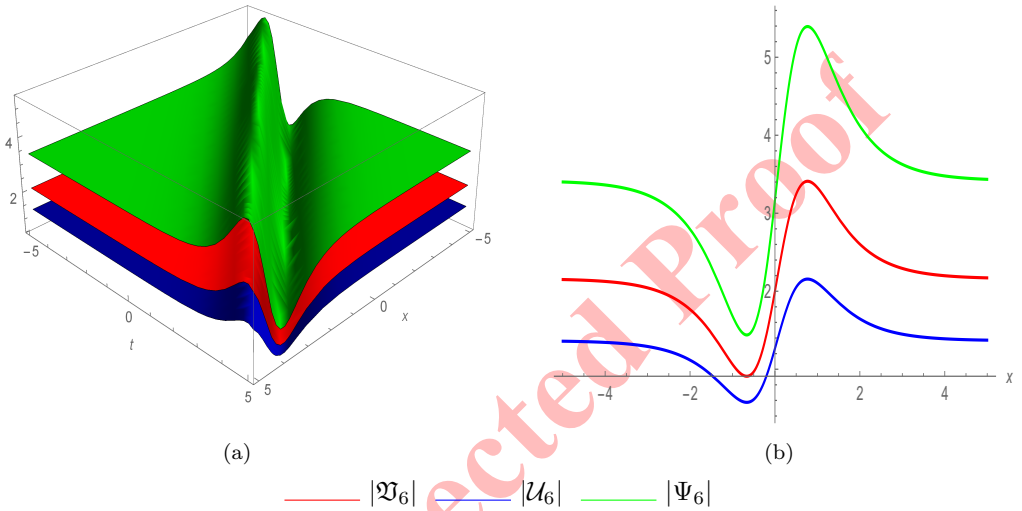

FIGURE 4. Plots of $|\mathfrak{V}_6|$, $|\mathcal{U}_6|$ and $|\Psi_6|$, with $\lambda=0.55$, $\varrho_1=-1$, $\varrho_2=0.6$, $\sigma=0.98$, $\vartheta=0.87$, $\rho=0$, $\varpi_2=1.5$, $\varpi_0=0.91$, and $y=1.7$. (a) Three-dimensional plot, (b) Two-dimensional plot.

$$\mathfrak{V}_7^{\pm}(\zeta)=\frac{\varrho_1\varpi_2-\sqrt{\varrho_1^2\varpi_2^2-3\varrho_0\varrho_2\varpi_2^2}}{3\varrho_2}+\left(\coth\left(\frac{\sqrt{-\varrho_1}}{2\sqrt{2}}(\rho+\zeta)\right)^2\pm\frac{\sqrt{-\frac{\varrho_1}{\varrho_2}}}{2\sqrt{2}}\right)^2\varpi_2\tanh\left(\frac{\sqrt{-\varrho_1}}{2\sqrt{2}}(\rho+\zeta)\right)^2, \tag{2.48}$$

$$\mathcal{U}_7^{\pm}(\zeta)=\frac{\lambda}{\vartheta}\mathfrak{V}_7^{\pm}(\zeta), \tag{2.49}$$

$$\Psi_7^{\pm}(\zeta)=\frac{\vartheta}{\lambda}\mathfrak{V}_7^{\pm}(\zeta). \tag{2.50}$$

$$\mathfrak{V}_8^{\pm}(\zeta)=\frac{\varrho_1\varpi_2-\frac{3\varrho_1\varpi_2\left(\sqrt{A_1^2+A_2^2}-A_1\cosh\left(\left(\sqrt{2}\sqrt{-\varrho_1}\right)(\rho+\zeta)\right)\right)^2}{2\left(A_1\sinh\left(\left(\sqrt{2}\sqrt{-\varrho_1}\right)(\rho+\zeta)\right)+A_2\right)^2}-\sqrt{\left(\varrho_1^2-3\varrho_0\varrho_2\right)\varpi_2^2}}{3\varrho_2}, \tag{2.51}$$

$$\mathcal{U}_8^{\pm}(\zeta)=\frac{\lambda}{\vartheta}\mathfrak{V}_8^{\pm}(\zeta), \tag{2.52}$$

$$\Psi_8^{\pm}(\zeta)=\frac{\vartheta}{\lambda}\mathfrak{V}_8^{\pm}(\zeta). \tag{2.53}$$

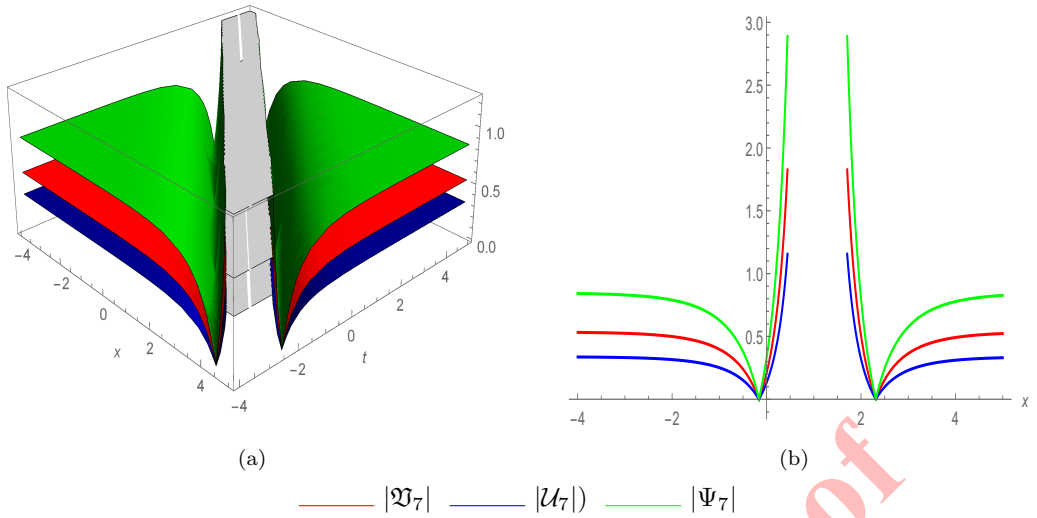

FIGURE 5. Plots of $|\mathfrak{V}_7|$, $|\mathcal{U}_7|$ and $|\Psi_7|$, with $\lambda = 0.55,\ \varrho_1 = -1,\ \varrho_2 = 2,\ \sigma = 0.98,\ \vartheta = -0.87,\ \rho = 0,\ \varpi_2 = 1.5,\ \varpi_0 = -0.91$, and $y = 1.7$. (a) Three-dimensional plot, (b) Two-dimensional plot.

$$\mathfrak{V}_9^{\pm}(\zeta) = \frac{-2\sqrt{(\varrho_1^2 - 3\varrho_0\varrho_2)\,\varpi_2^2} + \varrho_1\varpi_2\left(2 - \frac{3\cosh\left(\left(\sqrt{2}\sqrt{-\varrho_1}\right)(\rho+\zeta)\right)^2}{\left(\sinh\left(\left(\sqrt{2}\sqrt{-\varrho_1}\right)(\rho+\zeta)\right)\pm i\right)^2}\right)}{6\varrho_2}, \tag{2.54}$$

$$\mathcal{U}_9^{\pm}(\zeta) = \frac{\lambda}{\vartheta}\mathfrak{V}_9^{\pm}(\zeta), \tag{2.55}$$

$$\Psi_9^{\pm}(\zeta) = \frac{\vartheta}{\lambda}\mathfrak{V}_9^{\pm}(\zeta). \tag{2.56}$$

4. For $\varrho_0 = 0,\ \varrho_1 < 0$, and $\varrho_2 \neq 0$.
The trigonometric function solutions are the following:

$$\mathfrak{V}_{10}^{\pm}(\zeta) = \frac{\varrho_1\varpi_2 - 3\varrho_1\varpi_2\left(\sec\left(\sqrt{-\varrho_1}(\rho+\zeta)\right)\right)^2 - \sqrt{(\varrho_1^2 - 3\varrho_0\varrho_2)\,\varpi_2^2}}{3\varrho_2}, \tag{2.57}$$

$$\mathcal{U}_{10}^{\pm}(\zeta) = \frac{\lambda}{\vartheta}\mathfrak{V}_{10}^{\pm}(\zeta), \tag{2.58}$$

$$\Psi_{10}^{\pm}(\zeta) = \frac{\vartheta}{\lambda}\mathfrak{V}_{10}^{\pm}(\zeta). \tag{2.59}$$

$$\mathfrak{V}_{11}^{\pm}(\zeta) = \frac{\varrho_1\varpi_2 - 3\varrho_1\varpi_2\left(\csc\left(\sqrt{-\varrho_1}(\rho+\zeta)\right)\right)^2 - \sqrt{(\varrho_1^2 - 3\varrho_0\varrho_2)\,\varpi_2^2}}{3\varrho_2}, \tag{2.60}$$

$$\mathcal{U}_{11}^{\pm}(\zeta) = \frac{\lambda}{\vartheta}\mathfrak{V}_{11}^{\pm}(\zeta), \tag{2.61}$$

$$\Psi_{11}^{\pm}(\zeta) = \frac{\vartheta}{\lambda}\mathfrak{V}_{11}^{\pm}(\zeta). \tag{2.62}$$

5. For $\varrho_0 = \frac{\varrho_1^2}{4\varrho_2}, \varrho_1 > 0, \varrho_2 > 0$, and $A_1^2 - A_2^2 > 0$.

$$\mathfrak{V}_{12}^{\pm}(\zeta) = \frac{\varrho_1\varpi_2 + \frac{3}{2}\varrho_1\varpi_2\left(\tan\left(\frac{\sqrt{\varrho_1}}{\sqrt{2}}(\rho+\zeta)\right)\right)^2 - \sqrt{(\varrho_1^2 - 3\varrho_0\varrho_2)\,\varpi_2^2}}{3\varrho_2}, \tag{2.63}$$

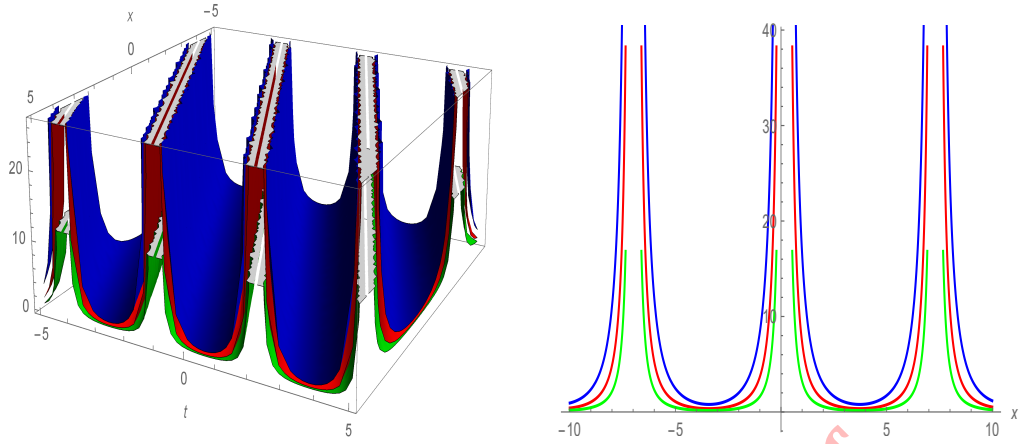

FIGURE 6. Plots of $|\mathfrak{V}_{11}|$, $|\mathcal{U}_{11}|$ and $|\Psi_{11}|$, with $\lambda = -1,\ \varrho_0 = 0,\ \varrho_1 = -1,\ \varrho_2 = 0.92,\ \sigma = 0.98,\ \vartheta = 0.44,\ \rho = 0.84,\ \varpi_2 = 0.96$, and $y = 0.91$. (a) Three-dimensional plot, (b) Two-dimensional plot.

$$\mathcal{U}_{12}^{\pm}(\zeta) = \frac{\lambda}{\vartheta}\mathfrak{V}_{12}^{\pm}(\zeta), \tag{2.64}$$

$$\Psi_{12}^{\pm}(\zeta) = \frac{\vartheta}{\lambda}\mathfrak{V}_{12}^{\pm}(\zeta). \tag{2.65}$$

$$\mathfrak{V}_{13}^{\pm}(\zeta) = \frac{\varrho_1\varpi_2 + \frac{3}{2}\varrho_1\varpi_2\left(\cot\left(\frac{\sqrt{\varrho_1}}{\sqrt{2}}(\rho+\zeta)\right)\right)^2 - \sqrt{(\varrho_1^2 - 3\varrho_0\varrho_2)\,\varpi_2^2}}{3\varrho_2}, \tag{2.66}$$

$$\mathcal{U}_{13}^{\pm}(\zeta) = \frac{\lambda}{\vartheta}\mathfrak{V}_{13}^{\pm}(\zeta), \tag{2.67}$$

$$\Psi_{13}^{\pm}(\zeta) = \frac{\vartheta}{\lambda}\mathfrak{V}_{13}^{\pm}(\zeta). \tag{2.68}$$

The mixed trigonometric function solutions are as below:

$$\mathfrak{V}_{14}^{\pm}(\zeta) = \frac{\varrho_1\varpi_2 + 3\varrho_2\varpi_2\left(\frac{\sqrt{\frac{\varrho_1}{\varrho_2}}\tan\left(\left(\sqrt{2}\sqrt{\varrho_1}\right)(\rho+\zeta)\right)}{\sqrt{2}} \pm \sec\left(\left(\sqrt{2}\sqrt{\varrho_1}\right)(\rho+\zeta)\right)\right)^2 - \sqrt{(\varrho_1^2 - 3\varrho_0\varrho_2)\,\varpi_2^2}}{3\varrho_2}, \tag{2.69}$$

$$\mathcal{U}_{14}^{\pm}(\zeta) = \frac{\lambda}{\vartheta}\mathfrak{V}_{14}^{\pm}(\zeta), \tag{2.70}$$

$$\Psi_{14}^{\pm}(\zeta) = \frac{\vartheta}{\lambda}\mathfrak{V}_{14}^{\pm}(\zeta). \tag{2.71}$$

$$\mathfrak{V}_{15}^{\pm}(\zeta) = \frac{\varrho_1\varpi_2 - \sqrt{\varrho_1^2\varpi_2^2 - 3\varrho_0\varrho_2\varpi_2^2}}{3\varrho_2} + \left(\frac{\sqrt{\frac{\varrho_1}{\varrho_2}}}{2\sqrt{2}} - \cot\left(\frac{\sqrt{\varrho_1}}{2\sqrt{2}}(\rho+\zeta)\right)^2\right)^2 \varpi_2\tan\left(\frac{\sqrt{\varrho_1}}{2\sqrt{2}}(\rho+\zeta)\right)^2, \tag{2.72}$$

$$\mathcal{U}_{15}^{\pm}(\zeta) = \frac{\lambda}{\vartheta}\mathfrak{V}_{15}^{\pm}(\zeta), \tag{2.73}$$

$$\Psi_{15}^{\pm}(\zeta) = \frac{\vartheta}{\lambda}\mathfrak{V}_{15}^{\pm}(\zeta). \tag{2.74}$$

$$\mathfrak{V}_{16}^{\pm}(\zeta)=\frac{\varrho_1\varpi_2+\frac{3\varrho_1\varpi_2\left(\sqrt{A_1^2-A_2^2}-A_1\cos\left(\left(\sqrt{2}\sqrt{\varrho_1}\right)(\rho+\zeta)\right)\right)^2}{2\left(A_1\sin\left(\left(\sqrt{2}\sqrt{\varrho_1}\right)(\rho+\zeta)\right)+A_2\right)^2}-\sqrt{\left(\varrho_1^2-3\varrho_0\varrho_2\right)\varpi_2^2}}{3\varrho_2}, \tag{2.75}$$

$$\mathcal{U}_{16}^{\pm}(\zeta)=\frac{\lambda}{\vartheta}\mathfrak{V}_{16}^{\pm}(\zeta), \tag{2.76}$$

$$\Psi_{16}^{\pm}(\zeta)=\frac{\vartheta}{\lambda}\mathfrak{V}_{16}^{\pm}(\zeta). \tag{2.77}$$

$$\mathfrak{V}_{17}^{\pm}(\zeta)=\frac{\varrho_1\varpi_2\left(\frac{3\cos\left(\left(\sqrt{2}\sqrt{\varrho_1}\right)(\rho+\zeta)\right)^2}{\left(\sin\left(\left(\sqrt{2}\sqrt{\varrho_1}\right)(\rho+\zeta)\right)\pm1\right)^2}+2\right)-2\sqrt{\left(\varrho_1^2-3\varrho_0\varrho_2\right)\varpi_2^2}}{6\varrho_2}, \tag{2.78}$$

$$\mathcal{U}_{17}^{\pm}(\zeta)=\frac{\lambda}{\vartheta}\mathfrak{V}_{17}^{\pm}(\zeta), \tag{2.79}$$

$$\Psi_{17}^{\pm}(\zeta)=\frac{\vartheta}{\lambda}\mathfrak{V}_{17}^{\pm}(\zeta). \tag{2.80}$$

6. For $\varrho_0=0$, and $\varrho_1>0$.
The exponential solutions are obtained as:

$$\mathfrak{V}_{18}^{\pm}(\zeta)=\frac{16\varrho_1^2\varpi_2e^{2\left(\pm\sqrt{\varrho_1}(\rho+\zeta)\right)}}{\left(4\varrho_1\varrho_2-e^{\pm2\sqrt{\varrho_1}(\rho+\zeta)}\right)^2}+\frac{\varrho_1\varpi_2-\sqrt{\varrho_1^2\varpi_2^2-3\varrho_0\varrho_2\varpi_2^2}}{3\varrho_2}, \tag{2.81}$$

$$\mathcal{U}_{18}^{\pm}(\zeta)=\frac{\lambda}{\vartheta}\mathfrak{V}_{18}^{\pm}(\zeta), \tag{2.82}$$

$$\Psi_{18}^{\pm}(\zeta)=\frac{\vartheta}{\lambda}\mathfrak{V}_{18}^{\pm}(\zeta). \tag{2.83}$$

$$\mathfrak{V}_{19}^{\pm}(\zeta)=\frac{16\varrho_1^2\varpi_2e^{2\left(\pm\sqrt{\varrho_1}(\rho+\zeta)\right)}}{\left(4\varrho_1\varrho_2e^{\pm2\sqrt{\varrho_1}(\rho+\zeta)}-1\right)^2}+\frac{\varrho_1\varpi_2-\sqrt{\varrho_1^2\varpi_2^2-3\varrho_0\varrho_2\varpi_2^2}}{3\varrho_2}, \tag{2.84}$$

$$\mathcal{U}_{19}^{\pm}(\zeta)=\frac{\lambda}{\vartheta}\mathfrak{V}_{19}^{\pm}(\zeta), \tag{2.85}$$

$$\Psi_{19}^{\pm}(\zeta)=\frac{\vartheta}{\lambda}\mathfrak{V}_{19}^{\pm}(\zeta). \tag{2.86}$$

3. Description of New Kudryashov's method

According to the new Kudryashov's method [41], Eq. (1.6) has following solution

$$\mathfrak{V}(\zeta)=\sum_{\sigma=0}^{\epsilon}\varpi_\sigma\phi^\sigma(\zeta), \tag{3.1}$$

where $\varpi_\epsilon\neq0$ and ϖ_σ are the coefficients that must be computed later for $\sigma=0,1,...,\epsilon$, and $\phi(\zeta)$ takes on the following form

$$\phi(\zeta)=\frac{4L}{4L^2e^{\delta\zeta}+\chi e^{-\delta\zeta}}, \tag{3.2}$$

where δ, χ and L are real values. Here, $\phi(\zeta)$ satisfies the subsequent equation

$$(\phi^{'}(\zeta))^2=\delta^2\phi^2(1-\chi\phi^2). \tag{3.3}$$

Inserting Eq. (3.3) along with Eq. (3.1) into Eq. (1.6), we begin our process by first finding ϵ by balancing rule.

3.1. **Solutions Strategy.** From Eq. (2.25), we get $\epsilon = 2$. Therefore, the solution takes the following form

$$\mathfrak{V}(\zeta) = \varpi_0 + \varpi_1\phi(\zeta) + \varpi_2\phi^2(\zeta). \tag{3.4}$$

Solution of Eq. (3.4) and the necessary derivatives are substituted into Eq. (2.25) to produce a polynomial. By collecting the coefficients of $\phi(\zeta)$ and equate them to zero, we have

$$\begin{aligned}
\lambda n\varpi_0^2 - 2\sigma\varpi_0 + \vartheta m\varpi_0^2 &= 0,\\
2\lambda\delta^2 l\vartheta^2\varpi_1 + 2\lambda n\varpi_0\varpi_1 - 2\sigma\varpi_1 + 2\vartheta m\varpi_0\varpi_1 &= 0,\\
8\lambda\delta^2 l\vartheta^2\varpi_2 + \lambda n\varpi_1^2 + 2\lambda n\varpi_0\varpi_2 - 2\sigma\varpi_2 + \vartheta m\varpi_1^2 + 2\vartheta m\varpi_0\varpi_2 &= 0,\\
-4\lambda\delta^2 l\vartheta^2\chi\varpi_1 + 2\lambda n\varpi_1\varpi_2 + 2\vartheta m\varpi_1\varpi_2 &= 0,\\
-12\lambda\delta^2 l\vartheta^2\chi\varpi_2 + \lambda n\varpi_2^2 + \vartheta m\varpi_2^2 &= 0.
\end{aligned} \tag{3.5}$$

Solving the above system, the following parameters are achieved

$$\varpi_0 = 0,\ \varpi_1 = 0,\ m = \frac{\lambda\left(12\delta^2 l\vartheta^2\chi - n\varpi_2\right)}{\vartheta\varpi_2},\ \sigma = 4\lambda\delta^2 l\vartheta^2. \tag{3.6}$$

The solution to Eq. (3.4) that corresponds to the parameters in Eq. (3.6), along with Eq. (3.3) is given

$$\mathfrak{V}^*(\zeta) = \frac{16L^2\varpi_2}{\left(4L^2e^{\delta\zeta} + \chi e^{\delta(-\zeta)}\right)^2}. \tag{3.7}$$

Solution (3.7) can be derived for $\chi = \pm 4L^2$, which leads to:

$$\mathfrak{V}_1^*(\zeta) = \frac{\varpi_2\mathrm{sech}^2(\delta\zeta)}{4L^2}, \tag{3.8}$$

$$\mathcal{U}_1^*(\zeta) = \frac{\lambda}{\vartheta}\mathfrak{V}_1^*(\zeta), \tag{3.9}$$

$$\Psi_1^*(\zeta) = \frac{\vartheta}{\lambda}\mathfrak{V}_1^*(\zeta), \tag{3.10}$$

and

$$\mathfrak{V}_2^*(\zeta) = \frac{\varpi_2\mathrm{csch}^2(\delta\zeta)}{4L^2}. \tag{3.11}$$

$$\mathcal{U}_2^*(\zeta) = \frac{\lambda}{\vartheta}\mathfrak{V}_2^*(\zeta), \tag{3.12}$$

$$\Psi_2^*(\zeta) = \frac{\vartheta}{\lambda}\mathfrak{V}_2^*(\zeta). \tag{3.13}$$

4. Simplest Equation Method

The key step in applying the SEM lies in selecting an appropriate simplest equation (SE). Here in [58], we choose the coupled Burgers' equation as it serves as a fundamental model for identifying solitary and multi-soliton solutions. Suppose, $\phi(\zeta)$ satisfies the following ODE

$$\phi_\zeta = \phi(\zeta) - \frac{1}{\vartheta}\phi(\zeta)^2. \tag{4.1}$$

Thus by using Hirota's method the general form of multi-soliton solution of (4.1) is derived as [39]:

$$\phi = \frac{\sum_{j=1}^{N}\vartheta_j e^{\vartheta_j x + \lambda_j y - \sigma_j t}}{1 + \sum_{j=1}^{N} e^{\vartheta_j x + \lambda_j y - \sigma_j t}}, \tag{4.2}$$

where ϑ_j, λ_j and σ_j are arbitrary constants.

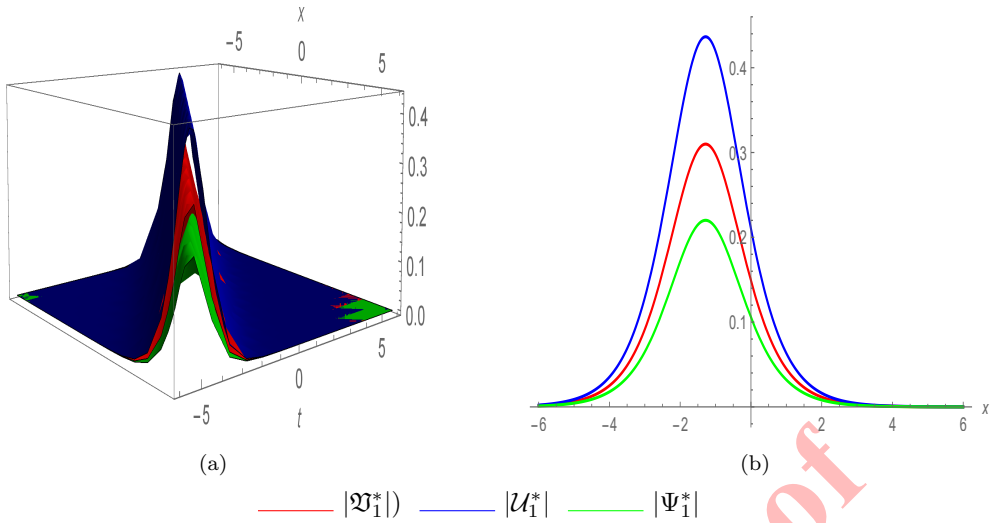

FIGURE 7. Plots of $|\mathfrak{V}_1^*|$, $|\mathcal{U}_1^*|$ and $|\Psi_1^*|$, with $\lambda = -1$, $\sigma = -0.98$, $\delta = 1$, $\vartheta = 0.71$, $L = 0.88$, $\chi = 0.93$, $\varpi_2 = -0.96$, and $y = -0.91$. (a) Three-dimensional plot, (b) Two-dimensional plot.

4.1. **Application of SEM.** By putting (2.27) and (4.1) into (2.25), we obtain the system of equations and by solving that system, the following values of constants are obtained

$$\varpi_0 = 0,\ \varpi_1 = \varpi_2(-\vartheta),\ l = \frac{\sigma}{\lambda\vartheta^2},\ n = \frac{\varpi_2(-m)\vartheta^3 - 12\sigma}{\varpi_2\lambda\vartheta^2}. \tag{4.3}$$

Now by substituting the above values in Eq. (2.27) then in Eq. (2.24), we have the following solutions

$$\mathfrak{V}_1^*(\zeta) = \varpi_1\left(\frac{\sum_{j=1}^{N}\vartheta_j e^{\vartheta_j x+\lambda_j y-\sigma_j t}}{1+\sum_{j=1}^{N} e^{\vartheta_j x+\lambda_j y-\sigma_j t}}\right) + \varpi_2\left(\frac{\sum_{j=1}^{N}\vartheta_j e^{\vartheta_j x+\lambda_j y-\sigma_j t}}{1+\sum_{j=1}^{N} e^{\vartheta_j x+\lambda_j y-\sigma_j t}}\right)^2, \tag{4.4}$$

$$\mathcal{U}_1^*(\zeta) = \frac{\lambda}{\vartheta}\mathfrak{V}_1^*(\zeta), \tag{4.5}$$

$$\Psi_1^*(\zeta) = \frac{\vartheta}{\lambda}\mathfrak{V}_1^*(\zeta). \tag{4.6}$$

For 1-Soliton solution, we have

$$\mathfrak{V}_{1,1}^*(\zeta) = \frac{\varpi_2\vartheta_1^2 e^{2(-t\sigma_1+x\vartheta_1+\lambda_1 y)}}{\left(e^{-t\sigma_1+x\vartheta_1+\lambda_1 y}+1\right)^2} - \frac{\varpi_2\vartheta_1^2 e^{-t\sigma_1+x\vartheta_1+\lambda_1 y}}{e^{-t\sigma_1+x\vartheta_1+\lambda_1 y}+1}, \tag{4.7}$$

$$\mathcal{U}_{1,1}^*(\zeta) = \frac{\lambda}{\vartheta}\mathfrak{V}_{1,1}^*(\zeta), \tag{4.8}$$

$$\Psi_{1,1}^*(\zeta) = \frac{\vartheta}{\lambda}\mathfrak{V}_{1,1}^*(\zeta). \tag{4.9}$$

For 2-Soliton solution, we have

$$\mathfrak{V}_{1,2}^*(\zeta) = \frac{\varpi_2\left(\vartheta_1^2 e^{2(-t\sigma_1+x\vartheta_1+\lambda_1 y)} + \vartheta_2^2 e^{2(-t\sigma_2+x\vartheta_2+\lambda_2 y)}\right)}{\left(e^{-t\sigma_1+x\vartheta_1+\lambda_1 y}+e^{-t\sigma_2+x\vartheta_2+\lambda_2 y}+1\right)^2} - \frac{\varpi 2\left(\vartheta_1^2 e^{-t\sigma_1+x\vartheta_1+\lambda_1 y}+\vartheta_2^2 e^{-t\sigma_2+x\vartheta_2+\lambda_2 y}\right)}{e^{-t\sigma_1+x\vartheta_1+\lambda_1 y}+e^{-t\sigma_2+x\vartheta_2+\lambda_2 y}+1}, \tag{4.10}$$

$$\mathcal{U}_{1,2}^*(\zeta) = \frac{\lambda}{\vartheta}\mathfrak{V}_{1,2}^*(\zeta), \tag{4.11}$$

$$\Psi_{1,2}^*(\zeta) = \frac{\vartheta}{\lambda}\mathfrak{V}_{1,2}^*(\zeta). \tag{4.12}$$

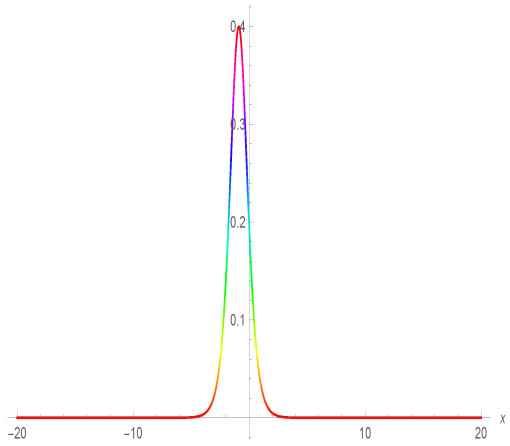

(a) 1-soliton

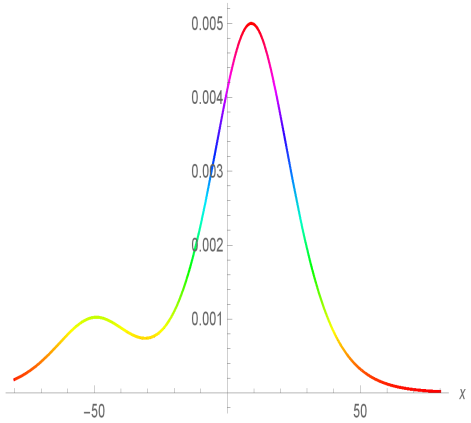

(b) 2-soliton

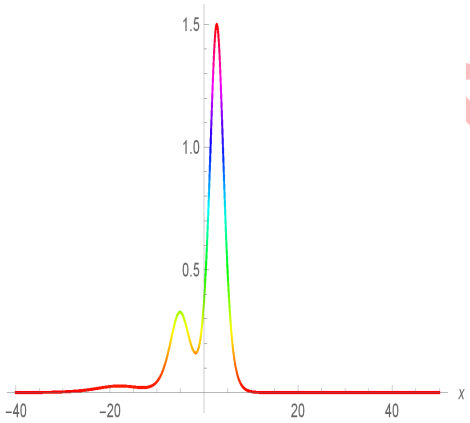

(c) 3-soliton

FIGURE 8. Soliton solutions with values $\varpi_2 = 1.2,\ \lambda_1 = 1,\ \lambda_2 = 0.7,\ \lambda_3 = 0.1,\ y = 0,\ \vartheta_1 = 1,\ \vartheta_2 = 2,\ \vartheta_3 = 0.3,\ \sigma_1 = 1,\ \sigma_2 = 0.7,\ \sigma_3 = 0.6.$

For 3-soliton

$$\mathfrak{V}^*_{1,3}(\zeta) = \frac{\varpi_2\left(\vartheta_1^2 e^{2(-t\sigma_1+x\vartheta_1+\lambda_1 y)} + \vartheta_2^2 e^{2(-t\sigma_2+x\vartheta_2+\lambda_2 y)} + \vartheta_3^2 e^{2(-t\sigma_3+x\vartheta_3+\lambda_3 y)}\right)}{\left(e^{-t\sigma_1+x\vartheta_1+\lambda_1 y} + e^{-t\sigma_2+x\vartheta_2+\lambda_2 y} + 1\right)^2} - \frac{\varpi_2\left(\vartheta_1^2 e^{-t\sigma_1+x\vartheta_1+\lambda_1 y} + \vartheta_2^2 e^{-t\sigma_2+x\vartheta_2+\lambda_2 y}\right)}{e^{-t\sigma_1+x\vartheta_1+\lambda_1 y} + e^{-t\sigma_2+x\vartheta_2+\lambda_2 y} + e^{(-t\sigma_3+x\vartheta_3+\lambda_3 y)} + 1}, \tag{4.13}$$

$$\mathcal{U}^*_{1,3}(\zeta) = \frac{\lambda}{\vartheta}\mathfrak{V}^*_{1,3}(\zeta), \tag{4.14}$$

$$\Psi^*_{1,3}(\zeta) = \frac{\vartheta}{\lambda}\mathfrak{V}^*_{1,3}(\zeta). \tag{4.15}$$

5. Stability analysis

This section examines the stability of the governing system using the Hamiltonian approach. The method is applied to specific solutions to evaluate their stability in different contexts [43]. Stability analysis is performed across various models. To analyze the stability of (1.3), we define the Hamiltonian transformation as follows:

$$\mathcal{M} = \frac{1}{2}\int_{-\infty}^{\infty} \mathfrak{V}^2\, dx. \tag{5.1}$$

In this context, $\mathcal{M}$ represents the momentum factor, while the potential for power is expressed by $\mathfrak{V}(x, y, t)$. We now establish a necessary criterion for the stability of soliton solutions:

$$\frac{\partial \mathcal{M}}{\partial \sigma} > 0, \tag{5.2}$$

where σ denotes the soliton velocity. By putting (3.8) into (5.1)

$$\mathcal{M} = \frac{1}{2}\int_{-10}^{10} \left(\frac{\varpi_2 \mathrm{sech}^2(\delta(-t\sigma + x\vartheta + \lambda y))}{4L^2}\right)^2 dx. \tag{5.3}$$

By using the criteria given in (5.2), we have

$$= -\frac{t\varpi_2\left(\mathrm{sech}^2(\delta(t\sigma - \lambda y + 10\vartheta)) - \mathrm{sech}^2(\delta(-t\sigma + \lambda y + 10\vartheta))\right)}{8L^2\vartheta} > 0. \tag{5.4}$$

Using the parameters $\delta = 0.6,\ \lambda = 3,\ L = 1,\ t = -1,\ y = 3,\ \varpi_2 = -2,\ \vartheta = -0.5$, and $\sigma = 0.6$, the solution remains stable. Thus, Equation (1.3) describes a stable nonlinear model, provided the specified condition is satisfied.

6. Semi-inverse variational principle

Over the past few decades, qualitative analysis and innovative mathematical techniques for addressing numerous nonlinear problems have been examined. The semi-inverse method [28, 42] is a potent and efficient approach for identifying variational principles in physical problems, offering valuable insight into the solution's nature.

According to Hes semi-inverse method [61], we construct the following trial-functional of Eq. (2.25)

$$J(\mathfrak{V}) = \int L d\zeta, \tag{6.1}$$

where L is an unknown function of $\mathfrak{V}$ and its derivatives.

Then, by the Ritz method, various forms of solitary wave solutions can be derived, including

$$\mathfrak{V}(\zeta) = Asech(B\zeta),\ \mathfrak{V}(\zeta) = Atanh(B\zeta),\ \mathfrak{V}(\zeta) = Acsch(B\zeta),\ \mathfrak{V}(\zeta) = Acoth(B\zeta). \tag{6.2}$$

Here, the parameters A and B represent the amplitude and inverse width of the soliton. SVP states that the parameters A and B can be retrieved from the coupled system of equations given by

$$\frac{\partial J}{\partial A} = 0, \tag{6.3}$$

and

$$\frac{\partial J}{\partial B} = 0. \tag{6.4}$$

6.1. **Application of SVP.** By the SVP, the subsequent variational formulation is established:

$$J = \int_0^{\infty} [3\vartheta^2 \lambda l \mathfrak{V}'^2 + \mathfrak{V}^3(\vartheta m + \lambda n) - 3\sigma \mathfrak{V}^2] d\zeta. \tag{6.5}$$

We look for a solitary wave solution using a Ritz-like technique in the form

$$\mathfrak{V}(\zeta) = A sech(B\zeta), \tag{6.6}$$

and so J, from (6.5), simplifies to

$$J = \frac{A^2\left(\pi A\vartheta m + \pi A\lambda n + 4B^2\vartheta^2\lambda l - 12\sigma\right)}{4B}. \tag{6.7}$$

Making J stationary with respect to A and B yields

$$\frac{\partial J}{\partial A} = \frac{A\left(3\pi A(\vartheta m + \lambda n) + 8\left(B^2\vartheta^2\lambda l - 3\sigma\right)\right)}{4B} = 0, \tag{6.8}$$

$$\frac{\partial J}{\partial B} = -\frac{A^2\left(\pi A(\vartheta m + \lambda n) - 4\left(B^2\vartheta^2\lambda l + 3\sigma\right)\right)}{4B^2} = 0. \tag{6.9}$$

By solving Eqs. (6.8) and (6.9), we get

$$A = \frac{48\sigma}{5\pi(\vartheta m + \lambda n)}, \; B = \frac{\sqrt{\frac{3}{5}}\sqrt{-\sigma}}{\vartheta\sqrt{\lambda}\sqrt{l}}, \tag{6.10}$$

which holds good for $\sigma < 0$. Hence finally, the solution to Eq. (1.3) is given by

$$\mathfrak{V}_* = \frac{48\sigma \operatorname{sech}\left(\frac{\sqrt{\frac{3}{5}}\sqrt{-\sigma}\zeta}{\vartheta\sqrt{\lambda}\sqrt{l}}\right)}{5\pi(\vartheta m + \lambda n)}, \tag{6.11}$$

$$\mathcal{U}_*(\zeta) = \frac{\lambda}{\vartheta}\mathfrak{V}^*_{1,2}(\zeta), \tag{6.12}$$

$$\Psi_*(\zeta) = \frac{\vartheta}{\lambda}\mathfrak{V}^*_{1,2}(\zeta). \tag{6.13}$$

7. Graphical behaviour and Numerical results

The objective of this section is to present numerical simulations of several exact solutions obtained utilizing the outlined methodologies. The applied methods have some advantages and limitations, which are summarized in Table 1.

Table 1. Comparison of methods: Advantages and limitations.

Method Name	Advantages	Limitations
Modified Sardar Sub-Equation Method (MSSEM)	Yields diverse solutions: dark, bright, singular, periodic-singular, and combined solitons.	Solutions depend on constraint conditions. Not applicable to first-order equations.
Simplest Equation Method (SEM)	Derives multisoliton solutions without altering the original NLPDE. Simple application without the need for bilinearization.	Limited to 1+1 dimensional equations.
New Kudryashov's Method	Gives hyperbolic solution in the form of dark, singular, bright and combined solution	Unable to derive periodic soliton solution
Semi-inverse variational method (SEM)	It can be used to establish generalized variational principles with multiple variables without the variational crisis phenomenon	The semi-inverse method's reliance on specific solution forms, like traveling waves or solitons, limits its generality when the true nature of the equation's solution differs.

The graphic representation of the results is a very strong and effective way to describe the nature of the obtained solutions and the relationship between all the parameters of the solutions. Hence, here a numerical simulation is

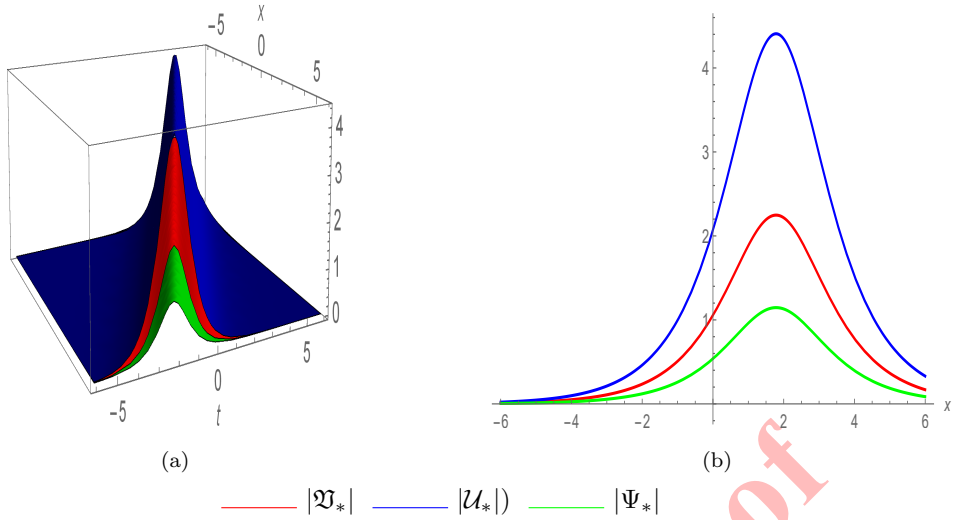

FIGURE 9. Plots of $|\mathfrak{V}_*|$, $|\mathcal{U}_*|$ and $|\Psi_*|$, with $\vartheta = 1,\ \lambda = 1,\ l = 0.99,\ m = 0.96,\ n = 0.87,\ \sigma = -1$, and $y = -0.91$. (a) Three-dimensional plot, (b) Two-dimensional plot.

performed and some 2D and 3D graphs of the obtained solutions are presented. It is significant to note that the characteristics of the wave profile are determined by the values of the associated parameters. We have illustrated several graphs of the solution for various free parameter values to help visualize the situation.

The 3D and 2D graphs in Figure 1 illustrate the bright solitary wave solutions of $|\mathfrak{V}_1|$, $|\mathcal{U}_1|$ and $|\Psi_1|$, where the parameters are set as $\lambda = -1,\ \varrho_0 = 0,\ \varrho_1 = 1,\ \varrho_2 = 0.92,\ \sigma = 0.98,\ \vartheta = 0.71,\ \rho = 0.84,\ \varpi_2 = 0.96$, and $y = 0.91$. In terms of functional solutions, the 2D line chart depicts higher and lower frequency and amplitudes. In Figure 2, the plots of the singular soliton solutions of $|\mathfrak{V}_2|$, $|\mathcal{U}_2|$ and $|\Psi_2|$ in 3D are depicted by choosing the following parametric values; $\lambda = -1,\ \varrho_0 = 0, \varrho_1 = 1,\ \varrho_2 = 0.92,\ \sigma = 0.98,\ \vartheta = 0.6,\ \rho = 0.84,\ \varpi_2 = 0.96$, and $y = 0.91$. Here, the function solutions in $|\mathfrak{V}_3|$, $|\mathcal{U}_3|$ and $|\Psi_3|$, $|\mathfrak{V}_|$, $|\mathcal{U}_5|$ and $|\Psi_5|$, $|\mathfrak{V}_8|$, $|\mathcal{U}_8|$ and $|\Psi_8|$ and $|\mathfrak{V}_9|$, $|\mathcal{U}_9|$ and $|\Psi_9|$ all show the same soliton solution form as obtained in hyperbolic function solutions. Also function solutions in $|\mathfrak{V}_{18}|$, $|\mathcal{U}_{18}|$ and $|\Psi_{18}|$, $|\mathfrak{V}_{19}|$, $|\mathcal{U}_{19}|$ and $|\Psi_{19}|$, $|\mathfrak{V}_{20}|$, $|\mathcal{U}_{20}|$ and $|\Psi_{20}|$ and $|\mathfrak{V}_{21}|$, $|\mathcal{U}_{21}|$ and $|\Psi_{21}|$ represent the singular soliton solutions that arise in exponential and rational function solutions. We just showed, for convenience, the solution shape for the function $|\mathfrak{V}_2|$, $|\mathcal{U}_2|$ and $|\Psi_2|$. In terms of functional solutions, the 2D line chart depicts higher and lower frequency and amplitudes. Figure 3 illustrates the dark soliton solutions of $|\mathfrak{V}_4|$, $|\mathcal{U}_4|$, and $|\Psi_4|$ in 3D by choosing the following parametric values; $\lambda = -1,\ \varrho_0 = 0.44,\ \varrho_1 = -1,\ \varrho_2 = 0.56,\ \sigma = -0.98,\ \vartheta = -0.85,\ \rho = -0.93,\ \varpi_2 = -1.5,\ \varpi_0 = 0.91$, and $y = -1.7$. In terms of functional solutions, the 2D line chart depicts higher and lower frequency and amplitudes. Figure 4 displays the dark-bright soliton solutions of $|\mathfrak{V}_6|$, $|\mathcal{U}_6|$, and $|\Psi_6|$ in 3D by choosing the following parametric values; $\lambda = 0.55,\ \varrho_1 = -1,\ \varrho_2 = 0.6,\ \sigma = 0.98,\ \vartheta = 0.87,\ \rho = 0,\ \varpi_2 = 1.5,\ \varpi_0 = 0.91$, and $y = 1.7$. In terms of functional solutions, the 2D line chart depicts higher and lower frequency and amplitudes.

Figure 5 illustrates the dark-singular soliton solutions of $|\mathfrak{V}_7|$, $|\mathcal{U}_7|$ and $|\Psi_7|$ in 3D by choosing the following parametric values; $\lambda = 0.55,\ \varrho_1 = -1,\ \varrho_2 = 2,\ \sigma = 0.98,\ \vartheta = -0.87,\ \rho = 0,\ \varpi_2 = 1.5,\ \varpi_0 = -0.91$, and $y = 1.7$. In terms of functional solutions, the 2D line chart depicts higher and lower frequency and amplitudes. In Figure 6, the plots of periodic soliton solutions of $|\mathfrak{V}_{11}|$, $|\mathcal{U}_{11}|$, and $|\Psi_{11}|$ in 3D and 2D are depicted by choosing the following parametric values; $\lambda = -1,\ \varrho_0 = 0,\ \varrho_1 = -1,\ \varrho_2 = 0.92,\ \sigma = 0.98,\ \vartheta = 0.44,\ \rho = 0.84,\ \varpi_2 = 0.96$, and $y = 0.91$. Here, the function solutions $|\mathfrak{V}_{10}|$, $|\mathcal{U}_{10}|$ and $|\Psi_{10}|$, $|\mathfrak{V}_{12}|$, $|\mathcal{U}_{12}|$ and $|\Psi_{12}|$, $|\mathfrak{V}_{13}|$, $|\mathcal{U}_{13}|$ and $|\Psi_{13}|$, $|\mathfrak{V}_{14}|$, $|\mathcal{U}_{14}|$ and $|\Psi_{14}|$, $|\mathfrak{V}_{15}|$, $|\mathcal{U}_{15}|$ and $|\Psi_{15}|$, $|\mathfrak{V}_{16}|$, $|\mathcal{U}_{16}|$ and $|\Psi_{16}|$, $|\mathfrak{V}_{17}|$, $|\mathcal{U}_{17}|$ and $|\Psi_{17}|$ are also depicts the same solution shape arises in trigonometric function solution. In terms of functional solutions, the 2D line chart depicts higher and lower frequency and amplitudes. Figure 7 demonstrates the bright soliton solution for $|\mathfrak{V}_1^*|$, $|\mathcal{U}_1^*|$, and $|\Psi_1^*|$ by choosing the following parametric values; $\lambda = -1,\ \sigma = -0.98,\ \delta = 1,\ \vartheta = 0.71,\ L = 0.88,\ \chi = 0.93,\ \varpi_2 =$

-0.96, and $y = -0.91$. In terms of functional solutions, the 2D line chart depicts higher and lower frequency and amplitudes. Figure 8 illustrates the 1-Soliton, 2-Soliton and 3-Soliton solutions for Eq. (1.3) with parameter values $\varpi_2 = 1.2,\ \lambda_1 = 1,\ \lambda_2 = 0.7,\ \lambda_3 = 0.1,\ y = 0,\ \vartheta_1 = 1,\ \vartheta_2 = 2,\ \vartheta_3 = 0.3,\ \sigma_1 = 1,\ \sigma_2 = 0.7,\ \sigma_3 = 0.6$. Figure 9 displays the bright soliton solutions of $|\mathfrak{V}_*|$, $|\mathcal{U}_*|$, and $|\Psi_*|$ in 3D by choosing the following parametric values; $\vartheta = 0.51,\ \lambda = 1,\ l = 0.99,\ m = 0.96,\ n = 0.87,\ \sigma = -1$, and $y = -0.91$.

8. Conclusion

In this article, optical soliton solutions to the Riemann wave equation are deduced with the assist of a modified Sardar sub-equation method, new Kudryashov method, Simplest equation method and Semi-inverse method. This leads to the depiction of a broad range of solutions with important physical perspectives and distinct dynamic behaviors, including bright solitons, dark solitons, singular solitons, combo bright-singular solitons, bright-dark soliton, periodic, exponential, rational, and multi-soliton solutions. These solutions offer valuable insights into various interesting wave properties, enhancing our understanding of the model. Furthermore, we harnessed the stability analysis of the solutions to provide a clearer study of the equation's dynamics. Solitary wave behavior has been graphically displayed with respect to both space and time. Numerical simulations of the specified outcomes were generated based on the selection of appropriate parametric values, and the intriguing physical patterns of the obtained solutions were displayed in 3D and 2D surfaces via Mathematica. It is clear from the graphs of the obtained solutions that our proposed methods are more authentic and efficient than other existing methods, producing more general solutions. The obtained solutions will be useful to investigate mathematical physics and engineering problems in more detail. This research will examine the practical implementation of the intended solutions as well as their physical interpretation. Future investigations into Riemann wave equation concerning solitary wave solutions can focus on advancements in numerical methods, analytical techniques, and the exploration of nonlinear dynamics, as well as interdisciplinary applications. Furthermore, exploring higher dimensions, nonlocal effects, and real-world complexities can enhance our comprehension and practical significance of solitary waves in diverse domains.

Declarations

Conflict of Interest. The authors declare that they have no conflict of interest.
Funding. The authors declare that no funds, grants, or other support were received during the preparation of this manuscript.
Data Availability. There is no data set used.

References

[1] M. J. Ablowitz, D. J. Kaup, A. C. Newell, and H. Segur, *Method for solving the sine-Gordon equation*, Physical Review Letters, *30*(25) (1973), 1262.
[2] M. J. Ablowitz, and H. Segur, *Solitons and the Inverse Scattering Transform*, SIAM, (1981).
[3] P. Agarwal, P. Varma, and M. Tiwari, *Study of gradient effects on kinetic Alfvn wave with inhomogeneous plasma*, Astrophysics and Space Science, *345* (2013), 99107.
[4] M. A. Akbar, N. H. M. Ali, and J. Hussain, *Optical soliton solutions to the (2+1)-dimensional ChaffeeInfante equation and the dimensionless form of the Zakharov equation*, Advances in Difference Equations, *2019*(1) (2019), 446.
[5] L. Akinyemi, M. enol, E. Az-Zobi, P. Veeresha, and U. Akpan, *Novel soliton solutions of four sets of generalized (2+1)-dimensional BoussinesqKadomtsevPetviashvili-like equations*, Modern Physics Letters B, *36*(01) (2022), 2150530.
[6] L. Akinyemi, M. enol, U. Akpan, and K. Oluwasegun, *The optical soliton solutions of generalized coupled nonlinear SchrdingerKortewegde Vries equations*, Optical and Quantum Electronics, *53* (2021), 114.
[7] L. Akinyemi, H. Rezazadeh, S.-W. Yao, M. A. Akbar, M. M. Khater, A. Jhangeer, M. Inc, and H. Ahmad, *Nonlinear dispersion in parabolic law medium and its optical solitons*, Results in Physics, *26* (2021), 104411.
[8] L. Akinyemi, U. Akpan, P. Veeresha, H. Rezazadeh, and M. n, *Computational techniques to study the dynamics of generalized unstable nonlinear Schrdinger equation*, Journal of Ocean Engineering and Science, (2022).

[9] E. A. Az-Zobi, W. A. Alzoubi, L. Akinyemi, M. enol, and B. S. Masaedeh, *A variety of wave amplitudes for the conformable fractional (2+1)-dimensional Ito equation*, Modern Physics Letters B, *35*(15) (2021), 2150254.

[10] C.-L. Bai, and H. Zhao, Complex hyperbolic-function method and its applications to nonlinear equations, Physics Letters A 355 (1) (2006) 3238.

[11] H. K. Barman, A. R. Seadawy, M. A. Akbar, and D. Baleanu, *Competent closed form soliton solutions to the Riemann wave equation and the NovikovVeselov equation*, Results in Physics, *17* (2020), 103131.

[12] H. K. Barman, M. S. Aktar, M. H. Uddin, M. A. Akbar, D. Baleanu, and M. Osman, *Physically significant wave solutions to the Riemann wave equations and the LandauGinsburgHiggs equation*, Results in Physics, *27* (2021), 104517.

[13] A. Biswas, Y. Yildirim, E. Yasar, Q. Zhou, S. P. Moshokoa, and M. Belic, *Optical solitons for Lakshmanan-PorsezianDaniel model by modified simple equation method*, Optik, *160* (2018), 2432.

[14] N. Cheemaa, A. R. Seadawy, and S. Chen, *More general families of exact solitary wave solutions of the nonlinear Schrdinger equation with their applications in nonlinear optics*, The European Physical Journal Plus, *133* (2018), 19.

[15] S. A. Elwakil, S. El-Labany, M. Zahran, and R. Sabry, *Modified extended tanh-function method for solving nonlinear partial differential equations*, Physics Letters A, *299*(23) (2002), 179188.

[16] A. El-Sayed, and P. Agarwal, *Spectral treatment for the fractional-order wave equation using shifted Chebyshev orthogonal polynomials*, Journal of Computational and Applied Mathematics, *424* (2023), 114933.

[17] X. Fan, T. Qu, S. Huang, X. Chen, M. Cao, Q. Zhou, and W. Liu, *Analytic study on the influences of higher-order effects on optical solitons in fiber laser*, Optik, *186* (2019), 326331.

[18] W. Gao, and H. M. Baskonus, *The modulation instability analysis and analytical solutions of the nonlinear GrossPitaevskii model with conformable operator and Riemann wave equations via recently developed scheme*, Advances in Mathematical Physics, (2023).

[19] C. Gu, and H. Hu, *Explicit solutions to the intrinsic generalization for the wave and sine-Gordon equations*, Letters in Mathematical Physics, *29*(1) (1993), 111.

[20] C. Gu, H. Hu, and Z. Zhou, *Darboux Transformations in Integrable Systems: Theory and Their Applications to Geometry*, Springer Science & Business Media, (2004).

[21] X. Guan, W. Liu, Q. Zhou, and A. Biswas, *Some lump solutions for a generalized (3+1)-dimensional KadomtsevPetviashvili equation*, Applied Mathematics and Computation, *366* (2020), 124757.

[22] A. Gurevich, A. Krylov, and G. El, *Evolution of a Riemann wave in dispersive hydrodynamics*, Zh. Eksp. Teor. Fiz, *101* (1992), 17971807.

[23] P. Hammachukiattikul, E. Sekar, A. Tamilselvan, R. Vadivel, N. Gunasekaran, and P. Agarwal, *Comparative study on numerical methods for singularly perturbed advanced-delay differential equations*, Journal of Mathematics, *2021*(1) (2021), 6636607.

[24] M. Hashemi, *Some new exact solutions of (2+1)-dimensional nonlinear Heisenberg ferromagnetic spin chain with the conformable time fractional derivative*, Optical and Quantum Electronics, *50*(2) (2018), 79.

[25] M. S. Hashemi, and D. Baleanu, *Lie Symmetry Analysis of Fractional Differential Equations*, CRC Press, (2020).

[26] T. Hayat, and M. Sajid, *Homotopy analysis of MHD boundary layer flow of an upper-convected Maxwell fluid*, International Journal of Engineering Science, *45*(28) (2007), 393401.

[27] J. He, *Variational iteration method for delay differential equations*, Communications in Nonlinear Science and Numerical Simulation, *2*(4) (1997), 235236.

[28] J.-H. He, *Semi-inverse method of establishing generalized variational principles for fluid mechanics with emphasis on turbomachinery aerodynamics*, International Journal of Turbo and Jet Engines, *14*(1) (1997), 2328.

[29] A. R. Helal, *BenjaminFeir instability in nonlinear dispersive waves*, Computers & Mathematics with Applications, *64*(11) (2012), 35573568.

[30] A. Houwe, S. Yakada, S. Abbagari, Y. Saliou, M. Inc, and S. Y. Doka, *Survey of third- and fourth-order dispersions including ellipticity angle in birefringent fibers on W-shaped soliton solutions and modulation instability analysis*, The European Physical Journal Plus, *136* (2021), 127.

[31] A. Houwe, S. Abbagari, Y. Saliou, M. Inc, S. Y. Doka, T. B. Bouetou, and M. Bayram, *Attitude of the modulation instability gain in oppositely directed coupler with the effects of the intrapulse Raman scattering and saturable function*, Results in Physics, *31* (2021), 104851.
[32] N. Irkl, E. Pikin, and P. Agarwal, *Global existence and decay of solutions for a system of viscoelastic wave equations of Kirchhoff type with logarithmic nonlinearity*, Mathematical Methods in the Applied Sciences, *45*(5) (2022), 29212948.
[33] A. Jeffrey, and M. Mohamad, *Exact solutions to the KdVBurgers equation*, Wave Motion, *14*(4) (1991), 369375.
[34] A. Jhangeer, H. Rezazadeh, and A. Seadawy, *A study of travelling, periodic, quasiperiodic and chaotic structures of perturbed FokasLenells model*, Pramana, *95* (2021), 111.
[35] K. Khan, and M. A. Akbar, *Exact and solitary wave solutions for the TzitzeicaDoddBullough and the modified KdVZakharovKuznetsov equations using the modified simple equation method*, Ain Shams Engineering Journal, *4*(4) (2013), 903909.
[36] M. M. Khater, M. Inc, R. A. Attia, D. Lu, and B. Almohsen, *Abundant new computational wave solutions of the GM-DP-CH equation via two modified recent computational schemes*, Journal of Taibah University for Science, *14*(1) (2020), 15541562.
[37] N. A. Kudryashov, *Method for finding highly dispersive optical solitons of nonlinear differential equations*, Optik, *206* (2020), 163550.
[38] P. R. Kundu, M. R. A. Fahim, M. E. Islam, and M. A. Akbar, *The sine-Gordon expansion method for higher-dimensional NLEEs and parametric analysis*, Heliyon, *7*(3) (2021).
[39] C.-K. Kuo, *The new exact solitary and multi-soliton solutions for the (2+1)-dimensional ZakharovKuznetsov equation*, Computers & Mathematics with Applications, *75*(8) (2018), 28512857.
[40] M. A. S. Murad, H. F. Ismael, F. K. Hamasalh, N. A. Shah, and S. M. Eldin, *Optical soliton solutions for time-fractional GinzburgLandau equation by a modified sub-equation method*, Results in Physics, *53* (2023), 106950.
[41] M. Ozisik, A. Secer, M. Bayram, and H. Aydin, *An encyclopedia of Kudryashovs integrability approaches applicable to optoelectronic devices*, Optik, *265* (2022), 169499.
[42] T. zi, and A. Yldrm, *Application of Hes semi-inverse method to the nonlinear Schrdinger equation*, Computers & Mathematics with Applications, *54*(78) (2007), 10391042.
[43] H. Qawaqneh, J. Manafian, M. Alharthi, and Y. Alrashedi, *Stability analysis, modulation instability, and beta-time fractional exact soliton solutions to the Van der Waals equation*, Mathematics, *12*(14) (2024).
[44] N. Savaissou, B. Gambo, H. Rezazadeh, A. Bekir, and S. Y. Doka, *Exact optical solitons to the perturbed nonlinear Schrdinger equation with dual-power law of nonlinearity*, Optical and Quantum Electronics, *52* (2020), 116.
[45] A. R. Seadawy, M. Arshad, and D. Lu, *The weakly nonlinear wave propagation theory for the KelvinHelmholtz instability in magnetohydrodynamics flows*, Chaos, Solitons & Fractals, *139* (2020), 110141.
[46] A. R. Seadawy, and B. A. Alsaedi, *Dynamical structure of optical soliton solutions and variational principle of nonlinear Schrdinger equation with Kerr law nonlinearity*, Modern Physics Letters B, *2024*, 2450254.
[47] A. R. Seadawy, and B. A. Alsaedi, *Variational principle and optical soliton solutions for some types of nonlinear Schrdinger dynamical systems*, International Journal of Geometric Methods in Modern Physics, *21*(6) (2024), 2430004245.
[48] A. R. Seadawy, and B. A. Alsaedi, *Variational principle for generalized unstable and modified unstable nonlinear Schrdinger dynamical equations and their optical soliton solutions*, Optical and Quantum Electronics, *56*(5) (2024), 844.
[49] A. R. Seadawy, D. Lu, and C. Yue, *Travelling wave solutions of the generalized nonlinear fifth-order KdV water wave equations and its stability*, Journal of Taibah University for Science, *11*(4) (2017), 623633.
[50] M. Shams, N. Rafiq, N. Kausar, P. Agarwal, C. Park, and N. A. Mir, *On highly efficient derivative-free family of numerical methods for solving polynomial equation simultaneously*, Advances in Difference Equations, *2021* (2021), 110.
[51] Y. Shang, *The extended hyperbolic function method and exact solutions of the longshort wave resonance equations*, Chaos, Solitons & Fractals, *36*(3) (2008), 762771.

[52] H. Triki, A. Yildirim, T. Hayat, O. M. Aldossary, A. Biswas, *Shock wave solution of the BenneyLuke equation*, Romanian Journal of Physics, *57*(78) (2012), 10291034.
[53] J. Vahidi, S. M. Zekavatmand, H. Rezazadeh, M. Inc, M. A. Akinlar, and Y.-M. Chu, *New solitary wave solutions to the coupled Maccari system*, Results in Physics, *21* (2021), 103801.
[54] M. Wadati, *The exact solution of the modified Kortewegde Vries equation*, Journal of the Physical Society of Japan, *32*(6) (1972), 16811681.
[55] X. Wang, *Exact and explicit solitary wave solutions for the generalised Fisher equation*, Physics Letters A, *131*(45) (1988), 277279.
[56] J. Wang, K. Shehzad, A. R. Seadawy, M. Arshad, and F. Asmat, *Dynamic study of multi-peak solitons and other wave solutions of new coupled KdV and new coupled ZakharovKuznetsov systems with their stability*, Journal of Taibah University for Science, *17*(1) (2023), 2163872.
[57] G. Wang, K. Yang, H. Gu, F. Guan, and A. Kara, *A (2+1)-dimensional sine-Gordon and sinh-Gordon equations with symmetries and kink wave solutions*, Nuclear Physics B, *953* (2020), 114956.
[58] A.-M. Wazwaz, *Multiple kink solutions for two coupled integrable (2+1)-dimensional systems*, Applied Mathematics Letters, *58* (2016), 16.
[59] Y. Yan, and W. Liu, *Stable transmission of solitons in the complex cubicquintic GinzburgLandau equation with nonlinear gain and higher-order effects*, Applied Mathematics Letters, *98* (2019), 171176.
[60] S.-W. Yao, L. Akinyemi, M. Mirzazadeh, M. Inc, K. Hosseini, and M. enol, *Dynamics of optical solitons in higher-order SasaSatsuma equation*, Results in Physics, *30* (2021), 104825.
[61] R. F. Zinati, and J. Manafian, *Applications of Hes semi-inverse method, ITEM and GGM to the DaveyStewartson equation*, The European Physical Journal Plus, *132* (2017), 126.
[62] Q. Zhou, L. Liu, H. Zhang, M. Mirzazadeh, A. H. Bhrawy, E. Zerrad, S. Moshokoa, and A. Biswas, *Dark and singular optical solitons with competing nonlocal nonlinearities*, Optica Applicata, *46*(1) (2016).